

Low-temperature transport properties of polycrystalline $\text{Ba}_8\text{Ga}_{16}\text{Sn}_{30}$

G.S. Nolas

Department of Physics, University of South Florida, Tampa, Florida 33620

J.L. Cohn

Department of Physics, University of Miami, Coral Gables, Florida 33124

J.S. Dyck and C. Uher

Department of Physics, University of Michigan, Ann Arbor, Michigan 48109

G.A. Lamberton, Jr. and T.M. Tritt

Department of Physics and Astronomy, Clemson University, Clemson, South Carolina 29634

(Received 17 June 2004; accepted 27 August 2004)

Low-temperature resistivity, Seebeck coefficient, thermal conductivity, and heat-capacity measurements were performed on $\text{Ba}_8\text{Ga}_{16}\text{Sn}_{30}$. This compound crystallizes in a cubic type-VIII clathrate phase, space group $I\bar{4}3m$, with the Ba atoms residing inside voids created by a tetrahedrally bonded network of Ga and Sn atoms. $\text{Ba}_8\text{Ga}_{16}\text{Sn}_{30}$ exhibits semiconducting behavior above 150 K with a low thermal conductivity and thus may hold potential for thermoelectric applications.

I. INTRODUCTION

Semiconducting group-IV clathrates have recently been identified as showing potential for thermoelectric applications.^{1,2} Most of the work to date investigating the transport properties of clathrate compounds has focused on clathrates with the type I clathrate crystal structure (space group $Pm\bar{3}n$). These compounds have the general formula $A_8B_yC_{46-y}$, where atoms B (Al, Zn, Cd, Ga, In) and C (Si, Ge, Sn) are tetrahedrally bonded to make a framework that forms cages in which the guest atoms A (Na, K, Rb, Cs, Sr, Ba, Eu) reside. The encapsulated atoms are said to “rattle” inside their atomic-sized cages, thus creating strong phonon-scattering centers. The localized vibrations of these atoms are believed to cause a dramatic lowering in the lattice thermal conductivity. Provided the electrical conduction takes place mostly through the frame, the rattling guest atoms will not greatly diminish the electrical conductivity. Indeed, semiconducting Ge-based clathrates exhibit lattice thermal conductivities typical of amorphous materials while maintaining good electronic properties.^{3,4} Materials of this type were described by Slack¹ as being “phonon-glass and electron-crystal” (PGEC) materials and meet one of the main criteria for finding new thermoelectric materials.

As part of a comprehensive study to assess the low-temperature transport properties of different clathrate

compounds and their potential for thermoelectric applications, we have synthesized $\text{Ba}_8\text{Ga}_{16}\text{Sn}_{30}$, a cubic material with the same general formula as that of type I clathrates but with a different crystal structure.⁵ In this report, we present low-temperature electrical and thermal transport measurements on $\text{Ba}_8\text{Ga}_{16}\text{Sn}_{30}$ and evaluate its potential for thermoelectric applications.

II. SAMPLE PREPARATION

Sample preparation consisted of mixing and reacting high-purity elements inside a pyrolytic boron nitride crucible, itself sealed inside a quartz ampoule, above the melting point of the constituents. The product was annealed for five days at 380 °C before removing from the furnace. The structural properties were analyzed by powder x-ray diffraction. The structure was identified as $I\bar{4}3m$ with a lattice constant of 11.600 Å. In this structure, the Ba atoms occupy cage voids created by the sp^3 hybridized network of Ga and Sn atoms. These cage voids can be thought of as distorted polyhedra connected by the (Ga,Sn) framework.⁵ Powder x-ray diffraction indicated trace amount of elemental Sn as a secondary phase. We note that our specimen had the type VIII crystal structure with no evidence of the type I clathrate crystal structure, as has been reported in the literature.⁶

The $\text{Ba}_8\text{Ga}_{16}\text{Sn}_{30}$ powders were ground to fine grains inside a glove box and hot pressed inside a graphite die at 380 °C and 2×10^4 lbs/in² for 2.5 h in an argon atmosphere. The resulting pellet had a density greater than 93% of the x-ray density. Optical metallographic

and electron-beam microprobe (XMP) analyses were performed on polished surfaces of the hot-pressed pellets. The average grain size was estimated to be $5.7 \mu\text{m}$.⁷ A thorough wavelength dispersive analysis indicated very small isolated grains of unreacted Sn among the $\text{Ba}_8\text{Ga}_{16}\text{Sn}_{30}$ grains. In some locations, unreacted Sn was also located between the $\text{Ba}_8\text{Ga}_{16}\text{Sn}_{30}$ grains. This trace amount of Sn was not observed throughout the pellet but only in some locations. The XMP analysis indicated the exact stoichiometry $\text{Ba}_8\text{Ga}_{15.8}\text{Sn}_{29.0}$, assuming the Ba sites are fully occupied. We note that this indicates vacancies on the (Ga,Sn) framework sites. Attempts to synthesize this compound with a varying Ga-to-Sn ratio, to vary the electronic properties as reported for type I Ge-clathrates,^{3,8} were not successful. The resulting compositions were basically $\text{Ba}_8\text{Ga}_{15.8}\text{Sn}_{29.0}$, as indicated by careful XMP analysis, while the transport properties of those specimens had values and temperature dependences similar to those we present below.

III. RESULTS AND DISCUSSION

The hot-pressed pellets were cut with a wire saw in the shape of a parallelepiped $2 \times 2 \times 5 \text{ mm}^3$ in size for transport measurements. Four-probe electrical resistivity (ρ), steady-state Seebeck coefficient (S), and steady-state thermal conductivity (κ) measurements were performed in a radiation-shielded vacuum probe. Heat losses via conduction through the lead wires and radiation were determined in separate experiments and the data corrected accordingly. Heat-capacity measurements were performed in the Quantum Design Physical Properties Measurement System (San Diego, CA) using the standard relaxation technique over the range of 2.2–350 K. The thermal coupling of the sample to the measurement stage was accomplished with a small amount of Apiezon N grease, and its contribution to the specific heat was measured in a separate experiment and subtracted from the final result.

Figure 1 shows S and ρ measurements from 300 to 5 K. The negative S values indicate electrons as majority carriers. The room temperature electron concentration, determined from Hall measurements, was $2.8 \times 10^{19} \text{ cm}^{-3}$. The magnitude of S increases with increasing temperature towards a modest value of $-137 \mu\text{V K}^{-1}$ at room temperature, a behavior typical of degenerately doped semiconductors. However, ρ exhibits a non-monotonic temperature dependence: a metallic-like behavior with $d\rho/dT > 0$ at low temperatures and a semiconducting-like dependence ($d\rho/dT < 0$) for $T > 150$ K. This latter behavior may be characterized by a simple activation-type conduction mechanism, with activation energy $E_a \sim 18 \text{ meV}$. Kuznetsov et al.⁹ reported a similar value of E_a (15 meV) for a specimen with similar electron concentration. The metallic-like behavior of ρ at $T < 150$ K indicates conduction in an impurity band. We

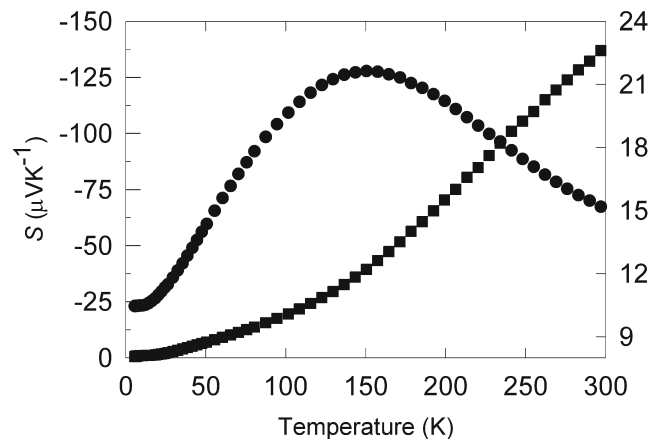


FIG. 1. Temperature dependent resistivity, in mohm-cm (circles), and Seebeck coefficient (squares) of $\text{Ba}_8\text{Ga}_{16}\text{Sn}_{30}$.

identify the activation energy of 18 meV as the energy difference between the impurity band and those in the conduction band.

Figure 2 shows the heat capacity as a function of temperature. The heat capacity C increases smoothly with temperature and shows typical Debye behavior. The Debye temperature, estimated to be 223 K, was calculated from a fit to the data at temperatures below 10 K, as shown in the inset in Fig. 2. The fit is extended in the inset to $T = 0$ to estimate γ ($= 1.26 \times 10^{-3} \text{ Jmol}^{-1} \text{ K}^{-2}$), the electronic contribution to the heat capacity where $C/T = \gamma + \alpha T^2$.¹⁰ Here γ and α correspond to the electronic and lattice contributions to the heat capacity, respectively.¹⁰ The estimated value for γ is within the range of values between pure metals and metal alloys.^{11,12}

Figure 3 shows the lattice thermal conductivity κ_L of $\text{Ba}_8\text{Ga}_{16}\text{Sn}_{30}$ along with a theoretical fit (solid line) to the data. The total thermal conductivity can be written as

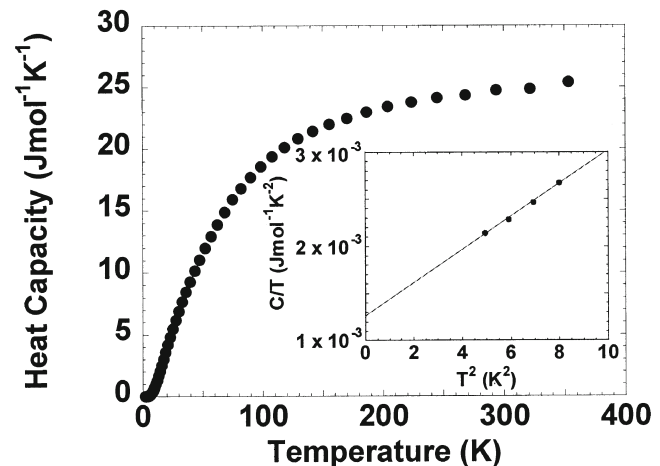


FIG. 2. Heat capacity of $\text{Ba}_8\text{Ga}_{16}\text{Sn}_{30}$ from 2.2 to 300 K. The inset shows the straight line fit of C/T versus T^2 for temperatures below 10 K used to estimate the Debye temperature.

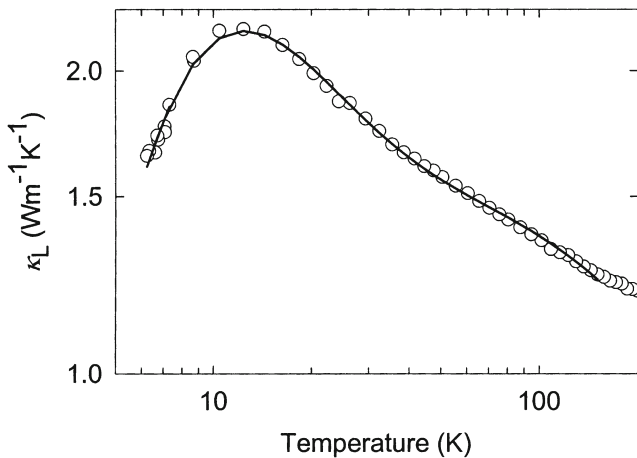


FIG. 3. Lattice thermal conductivity of $\text{Ba}_8\text{Ga}_{16}\text{Sn}_{30}$. The open circles are the experimental data and the solid line is a fit based on Eqs. (1) and (2).

$\kappa = \kappa_L + \kappa_e$. The electronic thermal conductivity κ_e was calculated using the Wiedemann–Franz relation ($\kappa_e = L_0 T / \rho$ with $L_0 = 2.45 \times 10^{-8} \text{ V}^2 \text{ K}^{-2}$) from the measured ρ . In this approximation the dominant contribution to the thermal conduction is from lattice phonons because at all temperatures κ_e is not more than 4% κ .

The thermal conductivity is similar in magnitude to (or smaller than) that of many compounds presently under investigation for thermoelectric applications.¹³ In fact, near room temperature the value ($\kappa_L = 1.1 \text{ W m}^{-1} \text{ K}^{-1}$) is similar to that of vitreous silica,¹⁴ a quintessential amorphous material. The temperature dependence of κ_L somewhat resembles that of a crystalline solid with a rising κ_L as temperature decreases leading to a peak at low temperatures. This rise in κ_L goes as $T^{-0.3}$ from approximately 25 to 15 K. This slow rise in κ_L with decreasing temperature indicates that “rattle” scattering of Ba may play a strong role on the phonon transport, along with other typical scattering mechanisms in dielectric solids. We explore the effect of the resonant “rattle” scattering contribution in theoretical modeling of the lattice thermal conductivity below.

The κ_L data were fit according to the equation¹⁵

$$\kappa_L(T) = \frac{k_B}{2\pi^2 v} \left(\frac{k_B T}{\hbar} \right)^3 \int_0^{\theta_D/T} \tau_c \frac{y^4 e^y}{(e^y - 1)^2} dy , \quad (1)$$

where ω is the phonon frequency, k_B is the Boltzmann constant, \hbar is the reduced Planck constant, y stands for the dimensionless parameter $y = \hbar\omega/k_B T$, θ_D is the Debye temperature, v is the velocity of sound, and τ_c is the combined phonon scattering relaxation time. This can be written as^{16,17}

$$\tau_c^{-1} = \frac{v}{L} + A\omega^4 + B\omega^2 T \exp\left(-\frac{\theta_D}{3T}\right) + C \frac{\omega^2 T^2}{[\omega^2 - \omega_0^2]^2} , \quad (2)$$

where the terms represent boundary, point defect (Rayleigh), phonon–phonon (Umklapp), and resonant scattering, respectively. Experimental values for θ_D (= 223 K) and L (= 5.7×10^{-6} m) were taken from specific heat data and optical metallographic analysis, respectively, while v , A , B , C , and ω_0 were used as fitting parameters. These values were 2984 m/s, $1.440 \times 10^{-41} \text{ s}^3$, $5.448 \times 10^{-18} \text{ s K}^{-1}$, $3.002 \times 10^{32} \text{ s}^{-3} \text{ K}^{-2}$, and $8.365 \times 10^{11} \text{ s}^{-1}$, respectively. Comparing the fitting parameters for Rayleigh and Umklapp scattering to that of another material of interest for thermoelectric applications, polycrystalline CoSb_3 ,¹⁶ A (the pre-factor for point defect scattering) is 50 times larger in the tin clathrate, while B is similar. This is reasonable, as we would expect alloy scattering due to the large number of vacancies on the framework sites suggested by our XPA analysis. The value for ω_0 is similar to that of Sr in $\text{Sr}_8\text{Ga}_{16}\text{Ge}_{30}$,¹⁷ indicating the possibility of resonance of the Ba vibrational modes with acoustic phonons in this compound. We note that attempts to fit the low-temperature data without the resonance scattering term proved unsuccessful. Further, the fact that only one resonant frequency is needed is consistent with the type-VIII clathrate structure in which there is only one cage size, unlike in the type-I structure, e.g., $\text{Sr}_8\text{Ga}_{16}\text{Ge}_{30}$, where there are two cage sizes and thus two frequencies¹⁷ are needed to describe the κ_L data.

IV. CONCLUSION

In summary, temperature-dependent electronic and thermal conductivity measurements on *n*-type Sn-clathrate with nominal composition $\text{Ba}_8\text{Ga}_{16}\text{Sn}_{30}$ have been reported. The κ values are low enough to make $\text{Ba}_8\text{Ga}_{16}\text{Sn}_{30}$ worthy of further investigations aimed at improving its thermoelectric performance. However, the electronic properties show a complex behavior. The ρ values are too high (by an order of magnitude) for this compound to be useful for thermoelectric applications. Thus the dimensionless figure of merit ($ZT = S^2/\rho\kappa$) at room temperature is only $ZT = 0.03$. Substitution of Zn or Cd instead of Ga and doping studies with Sb for *p*-type specimens, along with theoretical band-structure calculations, may help elucidate the electronic properties of this compound and guide their optimization for thermoelectric performance.

ACKNOWLEDGMENTS

G.S.N. gratefully acknowledges support from the University of South Florida. C.U. acknowledges support by Office of Natural Resources Grant No. N00014-03-1-0276.

REFERENCES

1. G.A. Slack: New materials and performance limits for thermoelectric cooling. In *CRC Handbook of Thermoelectrics*, edited by D.M. Rowe (CRC Press, Boca Raton, FL, 1995), p. 407.

2. G.S. Nolas, G.A. Slack, and S.B. Schjuman: Semiconductor clathrates: A phonon-glass electron-crystal material with potential for thermoelectric applications, in *Semiconductors and Semimetals*, Vol. 69, edited by T.M. Tritt (Academic Press, San Diego, CA, 2000) p. 255, and references therein.
3. G.S. Nolas, J.L. Cohn, G.A. Slack, and S.B. Schjuman: Semiconducting Ge clathrates: Promising candidates for thermoelectric applications. *Appl. Phys. Lett.* **73**, 178 (1998).
4. N.P. Blake, L. Mollnitz, G. Kresse, and H. Metiu: Why clathrates are good thermoelectrics: A theoretical study of $\text{Sr}_8\text{Ga}_{16}\text{Ge}_{30}$. *J. Chem. Phys.* **111**, 3133 (1999).
5. B. Eisenmann, H. Schafer, and R. Zagler: The compounds $\text{A}_8^{\text{II}}\text{B}_{16}^{\text{III}}\text{B}_{30}^{\text{IV}}$ ($\text{A}^{\text{II}} = \text{Sr, Ba}$, $\text{B}^{\text{III}} = \text{Al, Ga}$, $\text{B}^{\text{IV}} = \text{Si, Ge, Sn}$) and their cage structure. *J. Less-Common Met.* **118**, 43 (1986).
6. H.G. Schnering, W. Carrillo-Cabrera, R. Kroner, E-M. Petters, K. Peters, and R. Nesper: Crystal structure of the clathrate b- $\text{Ba}_8\text{Ga}_{16}\text{Sn}_{30}$. *Z. Kristallogr. - New Cryst.* **213**, 697 (1998).
7. E.E. Underwood: Quantitative metallography, in *Metallography and Microstructure*, Metals Handbook, 9th ed., Vol. 9 (American Society for Metals, Materials Park, OH, 1985), p. 123.
8. J.D. Bryan, N.P. Blake, H. Metiu, G.D. Stucky, B.B. Iverson, R.D. Poulsen, and A. Bentien: Nonstoichiometry and chemical purity effects in thermoelectric $\text{Ba}_8\text{Ga}_{16}\text{Ge}_{30}$ clathrate. *J. Appl. Phys.* **92**, 7281 (2002).
9. V.L. Kuznetsov, L.A. Kuznetsova, A.E. Kaliazin, and D.M. Rowe: Preparation and thermoelectric properties of $\text{A}_8^{\text{II}}\text{B}_{16}^{\text{III}}\text{B}_{30}^{\text{IV}}$ clathrate compounds. *J. Appl. Phys.* **87**, 7871 (2000).
10. N.W. Ashcroft and N.D. Mermin: *Solid State Physics* (Holt, Rinehart and Winston, Philadelphia, PA, 1976).
11. G.L. Guthrie, S.A. Friedberg, and J.E. Goldman: Specific heats of some copper-rich copper-nickel alloys at liquid helium. *Temp. Phys. Rev.* **113**, 45 (1959).
12. J. Rayne: Specific heats of metals below one degree absolute. *Phys. Rev.* **95**, 1428 (1954).
13. *Recent Trends in Thermoelectric Materials Research*, Vol. 69–71, edited by T.M. Tritt, in Semiconductors and Semimetals, Treatise Editors: R.K. Willardson and E.R. Weber (Academic Press, New York, 2001).
14. D.G. Cahill, S.K. Watson, and R.O. Pohl: Lower limit to the thermal conductivity of disordered crystals. *Phys. Rev. B* **46**, 6131 (1992).
15. J. Callaway: Model for lattice thermal conductivity at low temperatures. *Phys. Rev.* **113**, 1046 (1959).
16. J. Yang, G.P. Meisner, D.T. Morelli, and C. Uher: Iron valence in skutterudites: Transport and magnetic properties of $\text{Co}_{1-x}\text{Fe}_x\text{Sb}_3$. *Phys. Rev. B* **63**, 014410 (2000).
17. J.L. Cohn, G.S. Nolas, V. Fessatidis, T.H. Metcalf, and G.A. Slack: Glass-like heat conduction in high-mobility crystalline semiconductors. *Phys. Rev. Lett.* **82**, 779 (1999).